Waterborne polyester/clay@carbon dot nanocomposite for environmental remediation

Highlights

This chapter presents fabrication, characterization and property evaluation of eco-friendly high performing waterborne hyperbranched polyester (WHPE) nanocomposites with different doses of clay@carbon dot (CD) nanohybrid. The prepared nanohybrid and nanocomposite were characterized by different spectroscopic and analytical tools. XRD confirmed the absence of d_{001} reflections of bentonite clay, while TEM study revealed the partial exfoliation of the layers by the polyester chains. The thermoset of this nanocomposite with hyperbranched epoxy of glycerol (HBGE) and poly(amido amine) (PAA) showed an appreciable improvement in tensile strength, scratch hardness, impact resistance, Young's modulus, toughness and thermal stability compared to the pristine system. The nanocomposite also exhibited a high adsorption capacity for Pb(II) ions. Further, the nanocomposite was also used as a visible light active photocatalyst for removal of organic dye like Rodamine B (RhB). In addition, the nanocomposite exhibited biodegradability behavior against *Pseudomonus aerugionosa* bacterial strain. Thus, the nanocomposite is an exceptionally promising candidate as an environmentally friendly, low-cost and efficient material for elimination of organic and inorganic contaminants from the atmosphere.

This chapter is communicated to

Hazarika, D. and Karak, N. Nanocomposite of waterborne hyperbranched polyester and clay@carbon dot as a robust photocatalyst for environmental remediation. *Applied Surface Science (under revision)*

5.1. Introduction

Recent progress in nanotechnology have paid attention on development of nanohybrid by combination of two or more materials to achieve enhanced multi-functionality as well as generates materials with improved performance [1, 2]. Thus, in this study, hydrophilic nanoclay is directly combined with CD (as prepared) in the previous chapter without any modification in a single pot method and the nanohybrid was utilized for the fabrication of WHPE nanocomposites. The improvement in different properties like mechanical, physical, thermal, barrier, etc. have been extensively reported over the last two decades on incorporation of nanoclay into various polymers [3-5]. Clay is low cost and easily available green material as well as serves as a porous nanomaterial for the fabrication of polymer nanocomposite. Further, hydrophilic clay would be directly dispersed in waterborne polyester without any further modification [6, 7]. Such nanocomposite not only facilitates in enhancement of property but also supervised the environment because it is eco-friendly and non-toxic [7]. Literature reports a number of works on clay-based nanocomposites using different polymers such as epoxy resin, polystyrene, polyurethane, polyethylene, polyester, etc.[7-11] Among the great variety of clays, the use of bentonite is an interesting option as it can improve the adsorption capacity of the polyester, in addition to the above properties [12]. It is well recognized that certain metal ion disturbing their surface charge and interlayer complexation stability after entering into their crystal lattice [8, 9]. However, one of the major problems arise in the incorporation of this clay is the stable dispersion with required layers separation. On the other side of the coin, a perfectly exfoliated structure is very much essential to enrich the mechanical properties of the polyester [13]. Thus, to address this difficulty, a nanohybrid of clay with CD is aimed to prepare, as it possesses large number of polar functional groups which may interact both with the clay particles and polyester molecules along with some attractive attributes as mentioned in **Chapter 1**[14]. Further, the modification of clay with CD introduces photoluminescence (PL) property to the nanohybrid and thus incorporation of such nanohybrid into the polyester matrix may impart similar property to the nanocomposite [15]. Furthermore, though there are amply reports on clay-based solvent borne polyester nanocomposites [8, 12, 16] but WHPE/clay nanocomposite is rare to find. The hydroxylated dendritic polyester of 2,2-bis(hydroxy methyl) propionic acid (bis-MPA) and ethoxylated pentaerythrol with montmorillonite clay-based nanocomposite is reported by Decker *et al.* [17]. However, the study is only preliminary,

and no detail performance was available. The solvent borne biodegradable clay-based polyester nanocomposites were reported by Konwar *et al.* [16] and Lee *et al.* [18]. But, the mechanical properties of these nanocomposites are poor. Thus, to the best of our knowledge, there is no information about the fabrication and properties evaluation of WHPE/clay@CD nanocomposite. Thus, we aimed to fabricate such type of eco-friendly nanocomposites and tried to utilize them for adsorption of heavy metal ions (like Pb(II)) as release of such ions causes significant threat to the environment and public health. Here, it pertinent to mention that the adsorption is a commonly used method for removal of heavy metal ions owing to its cost-effective operation, simplicity of design and effortless insensitivity to toxic substances compared to other conventional methods. Again, Pb (II) containing effluents of textile and printing industries as well as other sources cause structural injure in the central nervous system, blood cells and mammalian eye [19]. Although many nanomaterials are reported for absorption of such metal ions, they suffer from ease of separation, reusability and non-biodegradabilty [20]. Again, an organic dye like RhB is another contaminant from similar effluents, which needs to be removed. Thus, the biodegradable polyester nanocomposite can be used for the purpose to overcome the above drawbacks.

Therefore, herein we have reported for the first time an environmentally pleasant nanocomposite of WHPE and clay@CD nanohybrid, fabricated through a facile and greener *in-situ* technique in absence of additional compatibilizing agent and organic solvent. The performance characteristics including biodegradability of the thermosetting nanocomposites were evaluated to examine the effect of nanohybrid loading on such attributes. Further, the wavelength dependent down- and up-conversion PL as well as anti-reflection property were also evaluated. Most importantly, it is aimed to use for removal of Pb(II) and RhB from the environment through adsorption and photocatalytic degradation, respectively.

5.2. Experimental

5.2.1. Materials

In this study, for fabrication of the nanocomposite WHPE50 was used as the matrix like previous chapter. WHPE50 was prepared by the same method using the same materials as described in **sub-Chapter 2B, sub-section 2B.2**.

The materials and method applied for preparation of CD was same as mentioned in the previous chapter.

Bentonite clay used for preparation of clay@CD nanohybrid was purchased from Sigma-Aldrich, Germany.

Lead (II) nitrate (purity ≥99) with molar mass 333.21 g mol^{-1}, density 4.53 g cm^{-3} and melting point 470 °C was purchased from Merck, India and used here for adsorption study.

RhB was obtained from Merck, India and used in this study for performing the photocatalytic test of the nanocomposite.

All other materials like solvents, HBGE, PAA, etc. required in this study were same as mentioned in the previous chapter.

5.2.2. Characterization

FTIR, XRD, TGA, DSC and SEM analyses, and mechanical tests were performed under the same conditions and by using the same instruments as described in **Chapter 3, section 3.2.2**. The morphology and SAED pattern of the nanohybrid and the nanocomposite were analyzed by the same HRTEM as mentioned in **Chapter 3, section 3.2.2**. The PL spectra of the nanocomposite were recorded using the same photoluminescent setup as mentioned in the previous chapter. Similarly, the transmittance of the nanocomposite films was evaluated by using same UV-visible spectrometer as mentioned in the previous chapter.

5.2.3. Preparation of clay@CD nanohybrid

Bentonite clay was first swelled in limited amount of water for around 12 h under constant magnetic stirring and heated at constant temperature of 70 °C. Then, equivalent amount CD as prepared in the previous chapter was mixed in the above solution and continued the stirring till it completely get dispersed.

5.2.4. Fabrication of WHPE/ clay@CD nanocomposite

Clay@CD-based WHPE nanocomposite was fabricated using bio-based raw materials through an environmental benign *in-situ* polymerization technique. The entire fabrication process was carried out without using any organic solvent, and compatabilizing agent which is in agreement to the principle of Green Chemistry. The first step of the fabrication process was the same as that of the pristine polyester, as described in **sub-Chapter 2A, sub-section 2A.2.2**. In the second step, clay@CD nanohybrid was also added along with bis-MPA and glycerol, and the reaction was continued at 140 °C until

desired product was obtained. Further, three different composition of the nanocomposite was fabricated using different doses of clay@CD nanohybrid (1, 2.5 and 5 wt%) by following the similar preparative procedure and encoded as PCCN1, PCCN2.5 and PCCN5, respectively.

5.2.5. Preparation of thermosetting nanocomposite

The thermosets of the nanocomposite was prepared by same method as described in **Chapter 2A, section 2A.4**.

5.2.6. Adsorption study

The nanocomposite was utilized for adsorption of Pb(II) and the experiment was performed by stirring a required amount of the adsorbent at room temperature in a predetermined concentration of Pb(II) solution (50 ppm). An aliquot of dispersed solution was withdrawn from the reaction mixture at different time intervals and recorded UV absorption. The removal percentage of heavy metal ion from the solution was calculated by the following equation [20, 21].

$$\text{Adsorption (\%)} = (C_0\text{-}C_e/C_0) \times 100 \quad \text{(Eq. 5.1)}$$

where C_o and C_e are the initial and final concentrations of the heavy metal ions.

Further, the adsorption capacity of Pb(II) was calculated using the following equation.

$$Q_e = (C_0\text{-}C_e) \times V/m \quad \text{(Eq. 5.2)}$$

where C_0 and C_e are the initial and equilibrium concentrations of Pb(II) (mg L^{-1}), V is the volume of the solution (L), and m is the mass of the nanocomposite (mg).

The adsorption kinetics was studied by using two kinetic models namely pseudo first order and pseudo second order [22]. The appropriateness of different models was established from the calculated correlation coefficient (R^2) and the value of R^2 more close to one specifies a more suitable model to the kinetics of adsorption of the metal ion. The equations for above two kinetic models are given below [22].

$$\log(q_e - q_t) = \log q_e - k_1 t/2.303 \quad \text{(Eq. 5.3)}$$

$$1/(q_e - q_t) = 1/q_e + k_2 t \quad \text{(Eq. 5.4)}$$

Further, during the adsorption process, the adsorption pattern between the adsorbed and the residual metal ions in the solution is illustrated by adsorption isotherm. Equilibrium isotherms are measured to find out the capacity of the adsorbent for metal ions. In this case, Langmuir and Freundlich models are the most common types of models describing this type of system [23].

Langmuir adsorption is based on the postulation that the highest adsorption corresponds to a saturated monolayer of solute molecules on the adsorbent surface and equation can be described by the linearized form as provided below.

$1/q_e = (1/q_m K_L)1/C_e + 1/q_m$ ..... (**Eq. 5.5**)

where C_e, q_e, q_m and k_L are equilibrium concentration of metal ions (mg/L), quantity of adsorbed metal ion (mg/g), monolayer adsorption capacity (mg/g) and equilibrium Langmuir constant (L/mg) respectively which signifies the nature of adsorption. The values of q_m and k_L were evaluated graphically from the plot of $1/q_e$ against $1/C_e$, which provides a straight line with intercept of $1/q_m$ and slope of $1/q_m k_L$.

The amount of adsorbate per unit mass of the adsorbent (q_e) was measured by Freundlich adsorption isotherm under equilibrium condition. This isotherm can be illustrated by the following equation [24].

$\log q_e = \log k_F + 1/n \log C_e$ ..... (**Eq. 5.6**)

where k_F and n are Freundlich constants and the values determined graphically. A plot of $\log q_e$ *vs* $\log C_e$ gives a straight line with slope 1/n and the intercept is $\log k_F$.

5.2.7. Anti-reflecting test

The anti-reflectance property of the thermosetting nanocomposite films was scrutinized by evaluating the value of transmittance, T (%) of them with the help of a UV-vis spectrophotometer.

5.2.8. Biodegradation study

The biodegradation study of the nanocomposites was carried out using the same bacterial strain by following the same procedure as described in **sub-Chapter 2A, sub-section 2A.2.8**.

5.2.9. Photocatalytic activity of the nanocomposite

RhB was chosen as model organic dirt in order to assess the photocatalytic ability of the nanocomposite. For this experiment, 100 mL aqueous solution of RhB (20 ppm) was exposed to sunlight for photodegradation in the presence of small pieces of nanocomposite films (0.05 g). The change in concentration of RhB was examined at specified time intervals by checking the UV absorbance intensity in the wavelength range of 300-700 nm. The rate of change of concentration of RhB with exposure time provided the photocatalytic activity of the films. The used pieces of nanocomposite in

the first cycle were taken out from the solution by normal filtration after achieving the maximum amount of degradation followed by washing and drying. Further, the weight of the dried films was taken and subsequently used to study the recyclability of the films. The rate of dye degradation was evaluated by plotting according to pseudo first order kinetic as follows [25].

$\ln C/C_0 = kt$ ..... (**Eq. 5.7**)

where, C_0, C and k are the initial concentration, concentration after time (t) of RhB and the first order rate constant.

5.3. Results and discussion

5.3.1 Preparation of the nanohybrid

In order to avoid the aggregation of clay particle in the polyester matrix, the nanohybrid of clay was prepared with CD. The strong interactions of polyester matrix with nanohybrid are likely to occur owing to the presence of large number of polar functional groups in CD. Thus it is expected that the dispersion as well as chance of exfoliation of clay by the polyester chains would be easier after the nanohybrid formation compare to the pristine clay. A preparative scheme of the nanohybrid is shown in **Scheme 5.1**.

FTIR spectra of bentonite clay and clay@CD nanohybrid are provided in **Figure 5.1a**. The characteristic bands observed at 1639, 529, 1035 and 1434 cm^{-1} are due to Si-O-Si, Si-O-Al, Si-O and Si-O-Si stretching vibrations respectively [26]. The bands appeared at 3470 and 3621 cm^{-1} are owing to symmetric and asymmetric stretching of freely bonded water molecules present on the surface of bentonite clay. In case of nanohybrid, the band for Si-O-Si stretching in the silicate galleries shifted from 1639 to 1626 cm^{-1} because of the interaction of CD and clay. The absence of bonded water molecules was confirmed by the absence of a band at around 3506-3602 cm^{-1} in the nanohybrid and hence increases the hydrophobicity, which consecutively offers good dispersion stability of the nanohybrid in different organic solvents [27]. FTIR study of nanohybrid evidently signified the strong interaction of CD with the bentonite clay, which consecutively influenced structural modifications in the bentonite. Further, the good interaction of CD and clay was also confirmed from shifting and decreasing of the reflection peak (d_{001}) at an angle 4.3° of bentonite clay in the XRD pattern of the nanohybrid (**Figure 5.1b**).

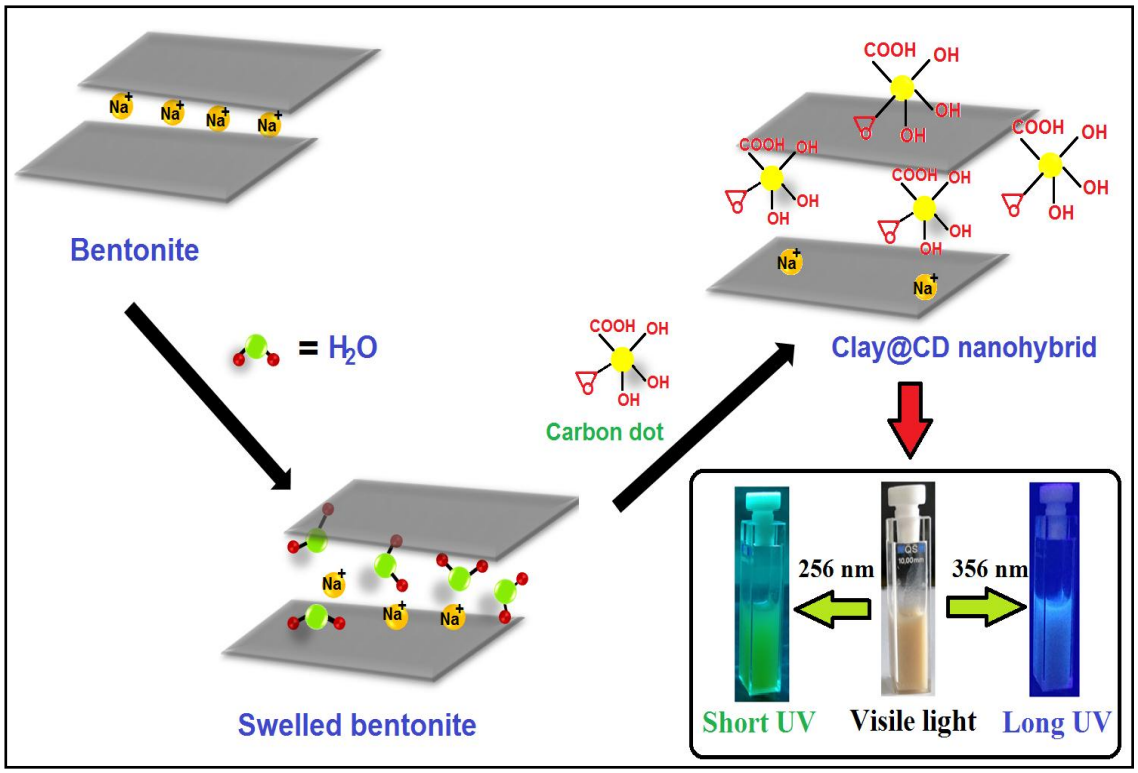

Scheme 5.1: Preparation of the nanohybrid

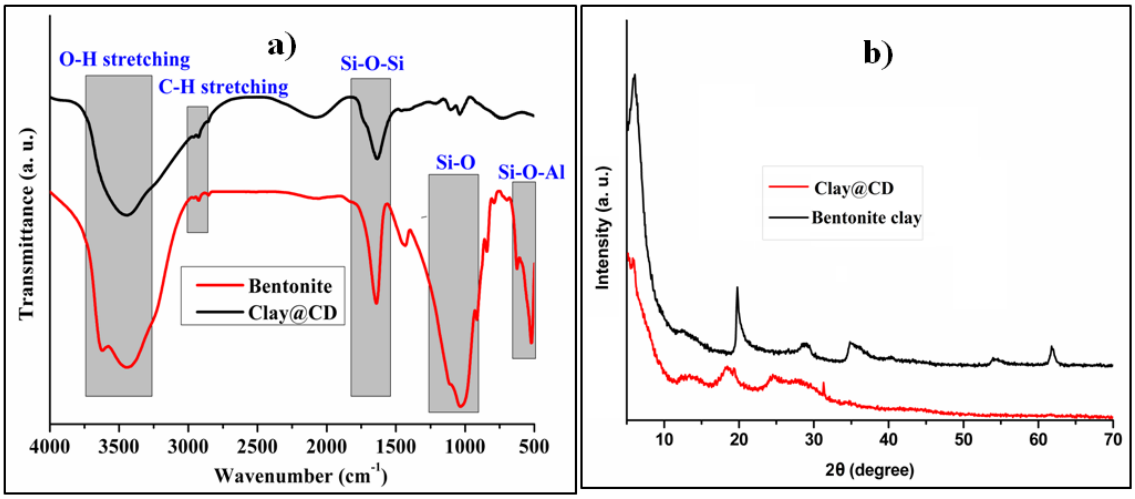

Figure 5.1: (a) FTIR spectra and **(b)** XRD patterns of bentonite clay and clay@CD nanohybrid

5.3.2. Fabrication and characterization of WHPE/CD@clay nanocomposite

WHPE nanocomposite was fabricated using clay@CD nanohybrid in absence of catalyst and compatibilizing agent. The mechanical shearing force during the fabrication process facilitated to mix the polyester matrix and the nanohybrid homogeneously. Nanoclay has the propensity of self-association to form aggregates owing to its higher activity and

large surface area. In this milieu, the polyester chains assist in delamination or exfoliation of clay layers by molecular interactions and diffusion [8]. This is due to the reason that the layers of nanoclay are stacked together with the aid of weak ionic force, which is further deteriorated by modification with organophilic functional groups. The carboxyl groups of the waterborne polyester can simply interact with hydroxyl groups of nanohybrid as well as negatively charged clay surface through H-bonding or other polar-polar interaction which develops a well dispersed and stable nanocomposites [8,16] (**Scheme 5.2**).

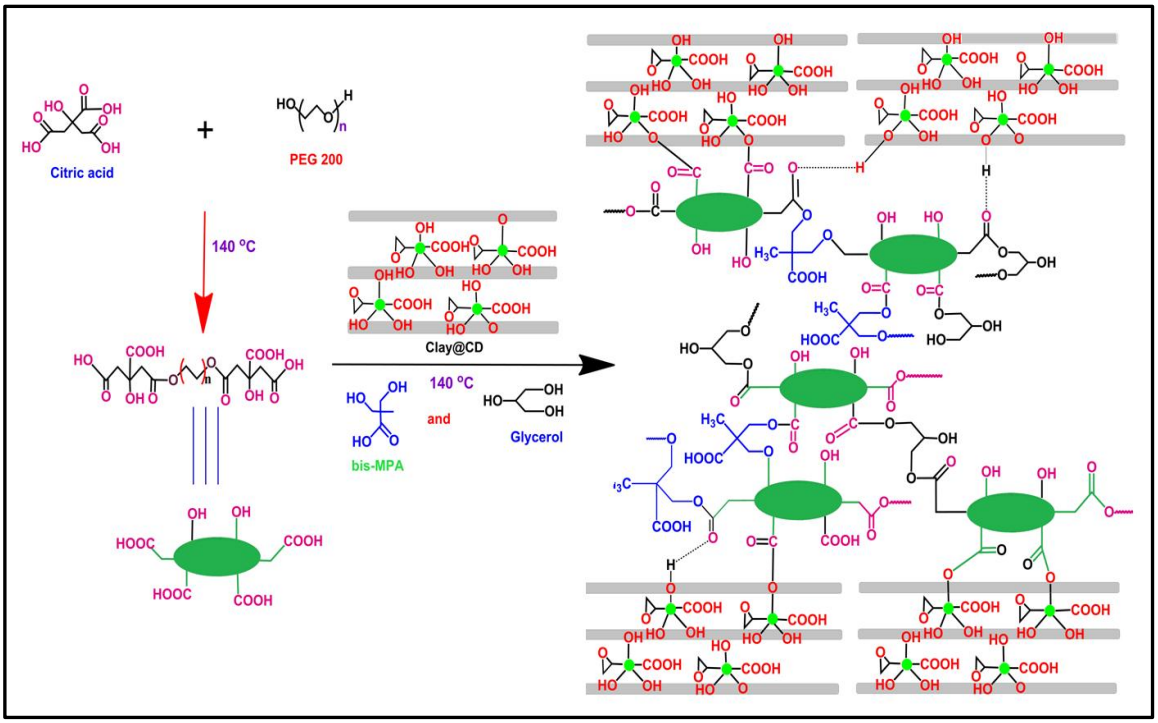

Scheme 5.2: Fabrication of clay@CD-based WHPE nanocomposite

Further, the nanocomposite was characterized by different spectroscopic techniques. In the FTIR spectra of nanocomposites (**Figure 5.2a**), nearly analogous characteristic bands like pristine polyester with the characteristic functional groups were noticed. However, the difference was noticed in the comparative intensity of the band at 1735 cm^{-1} (-C=O group) implies that -OH groups of the nanohybrid interact with -COOH and -OH groups of pristine polyester through H-bonding or other polar-polar interactions. The band for -OH stretching vibration (3422 cm^{-1}) of Al-OH and Si-OH moieties situated on the surface of clay shifted after formation of the nanocomposites to the lower wave number region (3410 cm^{-1}). This observation designates the existence of

interactions between -OH groups of the nanohybrid and -C=O and -OH groups of the polyester matrix [8, 16].

Further, in the XRD patterns of the nanocomposite (**Figure 5.2b**), the diminishing of diffraction peak for d_{001} confirmed the random dispersion and exfoliation of aluminosilicate layers of clay in the polyester matrix; which consecutively signifies the formation the nanocomposites with delaminated structure. This may be owing to the intercalation of polyester chain into the clay layers and the occurrence of strong interactions like H-bonding, polar-polar interactions, etc. [16]. These assist the fine dispersions of clay layers in the polyester matrix. Further, the broad peak observed at 20-30° was due to the amorphous nature of the polyester. Further, TEM study was conducted to understand the morphology of clay@CD nanohybrid inside the matrix and to evaluate the degree of dispersion. The representative TEM micrograph (**Figure 5.3**) of the nanocomposite (PCCN1) showed that the individual clay layers were found to be partially exfoliated or disintegrated and well dispersed in the polyester matrix.

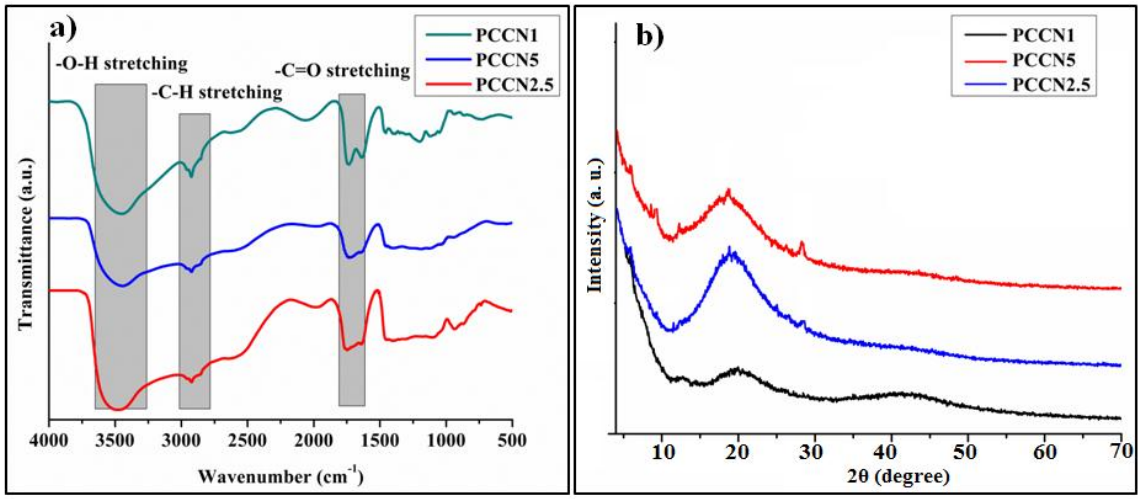

Figure 5.2: (a) FTIR spectra and **(b)** XRD patterns of the nanocomposites

This excellent distribution of the nanomaterials is due to the strong interaction occurred between the polar -COOH, -C=O, etc. groups of the waterborne polyester and the -OH groups of the nanohybrid. High surface functionality, globular and hyperbranched architecture of the waterborne polyester also contributed to the strong interactions [8, 27]. It is also observed from the TEM images that CD attached with the clay surface and well-separated from each other without aggregation. This is due to the strong physico-chemical interactions between the polar functional groups of polyester matrix and the

nanohybrid. The interlayer spacing between the clay platelets was found to be ~1.4 nm (**Figure 5.3**) because the polyester matrix intercalates the clay galleries by the strong interactions with the clay platelets and thereby assisting the process of immobilization.

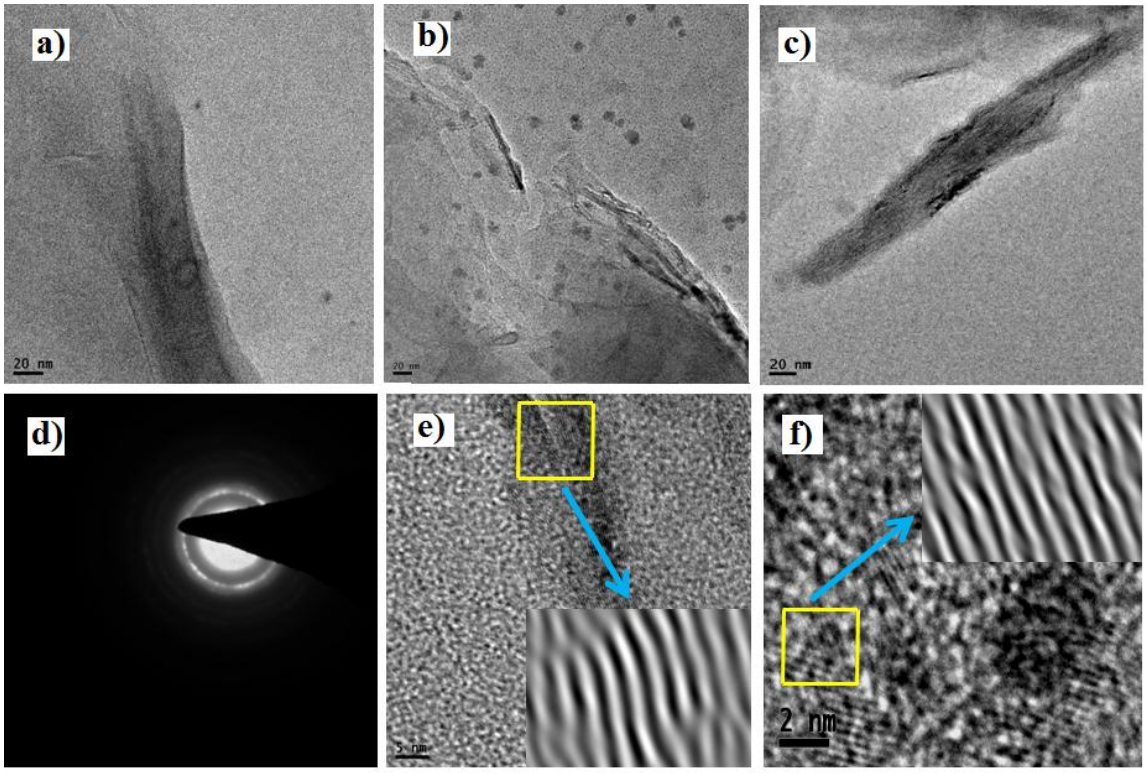

Figure 5.3: (a-c) Representative TEM images of PCCN1 at different magnification, **(d)** SAED pattern and **(e, f)** lattice fringes

5.3.3. Curing of the thermosets

The curing time decreased (5-3 h) after formation of the nanocomposite with increase in the loading of clay@CD (1-5 wt%). This decrease in curing time is due to the interaction of the clay layers with the polyester. Nanoclay, helps in physical cross-linking process through the formation of H-bonding between -OH groups of nanoclay and -OH/-COOH groups of polyester along with the epoxy group of hyperbranched epoxy and $-NH_2$ groups of PAA owing to the high surface area [8]. A variety of reactions were feasible during the curing process owing to the existence of a bulky number of reactive functional groups such as -OH, -C=O, -COOH and epoxy in the polyester matrix, epoxy, PAA and the nanohybrid. The free -OH groups of polyester and nanohybrid may interact with $-NH_2$ groups of PAA and the epoxide groups of epoxy. The ester and hydroxyl groups may react through transesterification reaction. Further, the hydrogen bonding was

formed between -C=O of polyester with the -OH of the epoxy and nanohybrid [8, 16]. Thus, the rate of curing of polyester nanocomposite enhanced with increase in the amount of the nanohybrid. The plausible interactions among waterborne polyester with epoxy and PAA during the cross-linking process are shown in **Scheme 5.3** through cartoon representation.

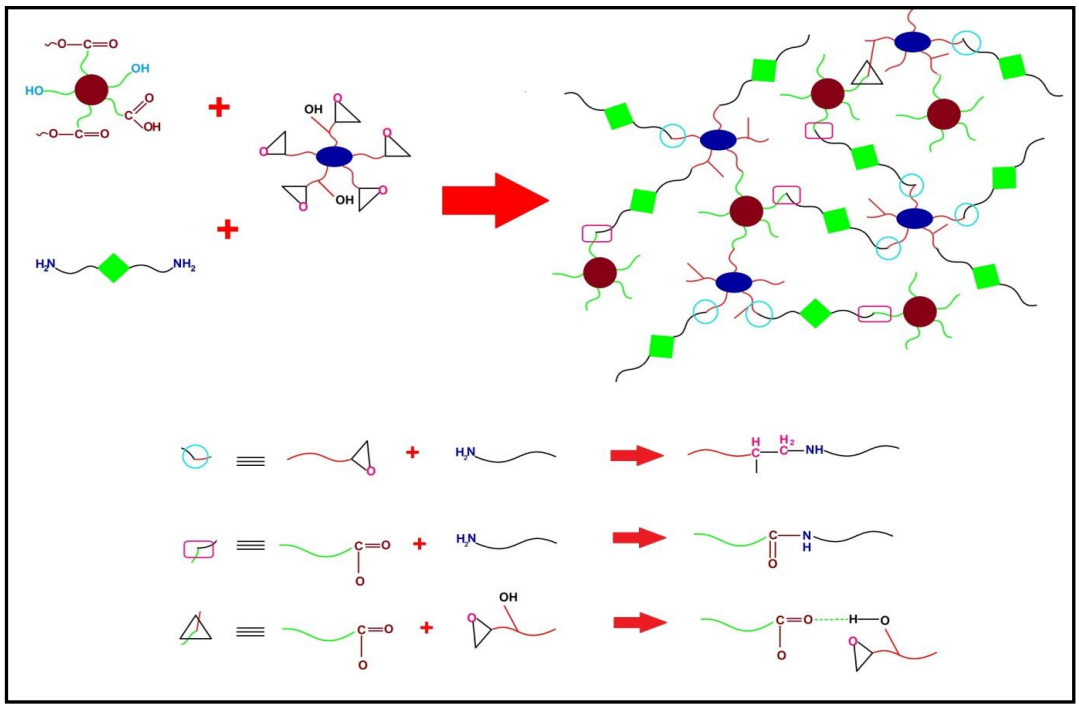

Scheme 5.3: Plausible interactions in the cross-linking process among the components

5.3.4. Performance characteristics

The mechanical properties like tensile strength, scratch hardness, elongation at break, toughness, etc. of the nanocomposites were evaluated and the results are given in **Table 5.1**. The incorporation of the nanohybrid showed excellent enhancement in such properties compared with the pristine polyester. This increment is attributed to the uniform distribution of the clay@CD nanohybrid and strong interactions as well as good interfacial adhesions with the polyester matrix. In addition, the well-dispersed nanohybrid itself opposes the tensile deformation and confines the segmental motions of the polymeric chains. The aspect ratio and orientation of clay could also influence the mechanical properties of the nanocomposites. The well dispersed nanoclay with high aspect ratio offer a higher stress-bearing capacity and added to the enhanced tensile strength as more surface area is available for interaction between clay layers and polymeric molecules [8, 16, 28]. The improvement in tensile strength may be also due to

the strong physical interactions among partially exfoliated clay platelets, quantum size CD and polyester matrix. The tensile strength of the waterborne polyester enhanced after formation of the nanocomposite and the values increased with increase in the loading of the nanohybrid because of well dispersion of the nanohybrid in the polyester matrix as well as good interaction with the matrix. The stress-strain profiles of the nanocomposites are provided in **Figure 5.4a**.

Table 5.1: Performance characteristics of the nanocomposite

Property	**PCCN0**	**PCCN1**	**PCCN2.5**	**PCCN5**
Tensile strength (MPa)	7.8 ± 1.8	19.9 ± 1.5	25 ± 2	35.7 ± 2.2
Elongation at break (%)	245 ± 3	270 ± 4	252 ± 4	171 ± 2
Scratch hardness (kg)	4 ± 0.5	5.5 ± 1	7.5 ± 0.5	>10
Impact resistance (kJ m^{-1})*	>8.3	>8.3	>9.5	>10
Toughness (MJ m^{-3})[a]	17.18 ± 3.5	38.12 ± 4.2	52.46 ± 3.8	49.89 ± 5
Gloss (°)	80 ± 2	85 ± 1	90 ± 2	93 ± 2
Young's modulus (MPa)	243 ± 3	290 ± 4	320 ± 3	340 ± 5

** Maximum limit of the instrument [a] Area under stress-strain profiles*

It is noticed from this figure that among all the thermosetting nanocomposites, PCCN5 exhibited the highest tensile strength owing to the presence of the highest amount of the nanohybrid. The observed values of tensile strength were found to be superior to the reported values of highly branched polyester/clay (4.53-11.8 N mm^{-2}) [16], aliphatic polyester/cloisoite 10A (11.99-12.45 MPa) [18], chitosan/nanoclay (4.42-14.40 MPa) [29], blended clay-based epoxy/polyester (20.71-25.81 MPa) [30] nanocomposites, etc. Further, the elongation at break of the nanocomposites also increased upon incorporation of the nanohybrid but the value dropped with increase in the loading of the nanohybrid. This is because of restricted motion of the polymeric chains at high loading of the clay layers. These elongation at break values were superior to the reported solvent borne polyester nanocomposites of montmorilonite clay (32.4-62.5 %), cloisite 30 B (12.45-22.25 %), etc. [16, 18]. Further, the toughness of the nanocomposites as determined by integrating the stress-strain curves was sharply increased with the increase of amount of the nanohybrid and the values dropped at 5 wt% loading as it is a combination of stress and strain. The increase in toughness is owing to the combined effects of the flexible

long hydrocarbon chains of aliphatic PAA and various flexible moieties of WHPE as well as epoxy with clay platelets and rigid moieties [16]. The plasticizing effect of these flexible moieties has specific role for these above results. Hence, scratch hardness and impact resistance related to toughness also improved after the formation of the nanocomposite owing to the formation of effective network through physical cross-linking. The homogeneously dissimilated nanoclay confines the indentation and improves the scratch hardness values [16]. Further, the gloss values increased with increase in the loading of clay from 1 to 5 wt% in the nanocomposite.The optimum cross-linking of the cured thermosets occurred in the nanocomposite which leads to the development of dimensionally smooth surface with the increase of clay loading [16].

5.3.5. Thermal properties

The thermal stability of the pristine polyester was improved after the formation of the nanocomposites with the incorporation of 1-5 wt% of the nanohybrid. The controlled mobility of the polymeric chains has strong effect in enrichment in the thermostability of the nanocomposites owing to the presence of intercalated clay galleries by the polymer chains. Further, another explanation for this increment is the constrained segmental motion of the polymeric chains. A diffusion effect is also happened by the inclusion of nanohybrid which forms char and obstructs the discharge of the volatile decomposition products. More char is formed with increase in the loading of the nanohybrid and thus promoted the thermal stability of the nanocomposites [16]. Further, heat insulating and mass transport barrier character of clay delay the escaping tendency of the volatiles, produced during decomposition process. The improvement in thermal stability is also because of the sturdy interactions of the nanohybrid with hyperbranched polyester, epoxy and PAA. Further, the quantum size of CD offers large surface area for such interactions as well as the presence of peripheral polar functional moieties and its aromatic carbonized structure provides strong physico-chemical interactions with the polyester matrix, which also improve the thermal stability of nanocomposites [31]. The nanocomposites were degraded by a two-step process, where the first step of degradation (242-260 °C) is due to degradation of aliphatic moieties while the second stage (~420 °C) is owing to degradation of aromatic moieties (**Figure 5.4b**).

5.3.6. Biodegradation study

The biodegradation efficacy of the thermosetting nanocomposite was checked by directly

exposing them to *Pseudomonus aeregunosa* bacterial strain. The bacterial growth curves illustrate the degradation of the nanocomposites which was achieved by measuring the optical density of the bacterial medium at 600 nm (**Figure 5.5**). An evident improvement in bacterial growth was realized in case of the nanocomposites and growth was further enhanced with the increment in the dose of the nanohybrid. This increment may be owing to the catalytic role of the clay in the biodegradation process. The degradation of polyester is a multifaceted process which chiefly involves four facts: absorption of water from polyester matrix; cleavage of ester linkages and formation of oligomeric fragments like monomeric carboxylic acids and diols; surface erosion owing to solubilization of oligomeric fragments; and diffusion of soluble oligomers by bacteria to generate CO_2, H_2O and humus.

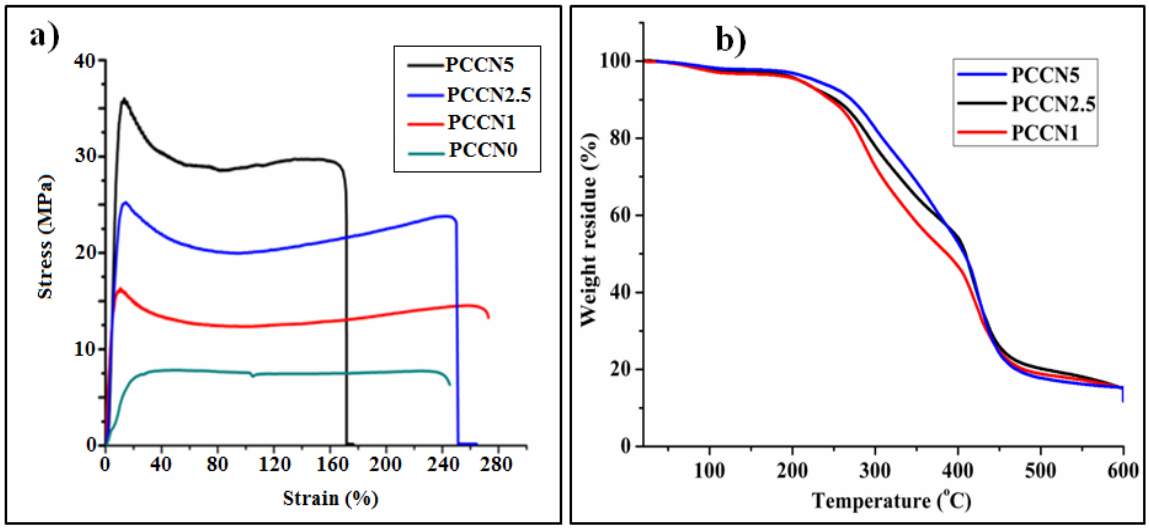

Figure 5.4: (a) Stress-strain profiles and **(b)** TGA thermograms of the thermosetting nanocomposite

Thus, any reason which enhances the hydrolysis tendency of polyester controls the degradation process. Further, the occurrence of terminal -OH groups of CD and the nanoclay layers may be accountable for this better biodegradation behavior of the nanocomposite. In case of nanocomposite, the partly exfoliated layers of nanoclay are uniformly dispersed in the polyester matrix and the -OH groups of nanoclay after absorbing water initiate heterogeneous hydrolysis of the polyester matrix [8, 16]. The representative SEM micrographs (**Figure 5.5**) of the nanocomposite after four weeks of bacterial exposure further confirmed the biodegradation abilities of the nanocomposites.

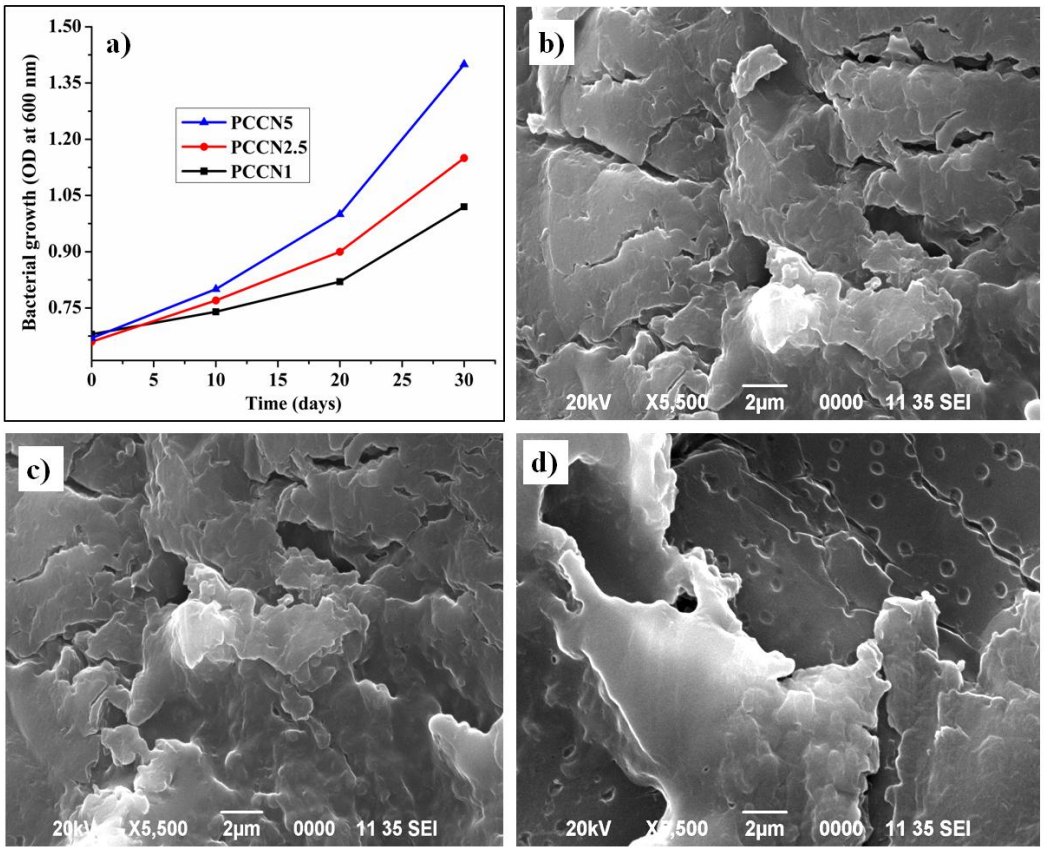

Figure 5.5: (a) Bacterial growth curves of the nanocomposites against *Pseudomonus aerogunosa* bacterial strain, and **(b, c)** SEM images of the degraded PCCN1 and **(d)** PCCN5

5.3.7. Optical properties

One of the most attractive properties of the nanocomposite was the ability to exhibit anti-reflective behavior which was yet not reported in literature for clay-based WHPE nanocomposite. The anti-reflectance behavior of the nanocomposite was confirmed from the obtained transmittance value as measured by UV-vis spectral study (**Figure 5.6a**). The nanocomposite containing 2.5 and 5 wt% of nanohybrid (PCCN2.5 and PCCN5) showed the transmittance values within the range of 80-88%. Further, the films of nanocomposite are still transparent and the maintenance of high transparency is because of smaller particle size and the uniform film morphology without pores and aggregates. Transparency arises in clay-based polymer nanocomposites owing to isotopic transmission of light caused by individual clay platelets either in semi or fully exfoliated state [32]. The excellent transmittance of the nanocomposite is due to the anti-reflecting properties of the thermosets, contributing to the reduction of the effective refractive index of the thermosets.

Further, this clay-based nanocomposite also exhibited both wavelength dependent down- and up-conversion PL properties owing to the presence of CD. The nanocomposite showed emission spectra in the region of 440-510 nm (**Figure 5.6b**) upon excitation from 330 to 410 nm, confirmed the wavelength dependent down-conversion property. While, upon exciting the nanocomposite in the wavelengths from 700 to 800 nm corresponding emission spectra were appeared from 440 to 540 nm (**Figure 5.6c**) which confirmed the wavelength dependent up-conversion property. This feature may be attributed to the various emissive sites and distribution of different particle sizes of the nanohybrid as well as to active multi-photon processes.

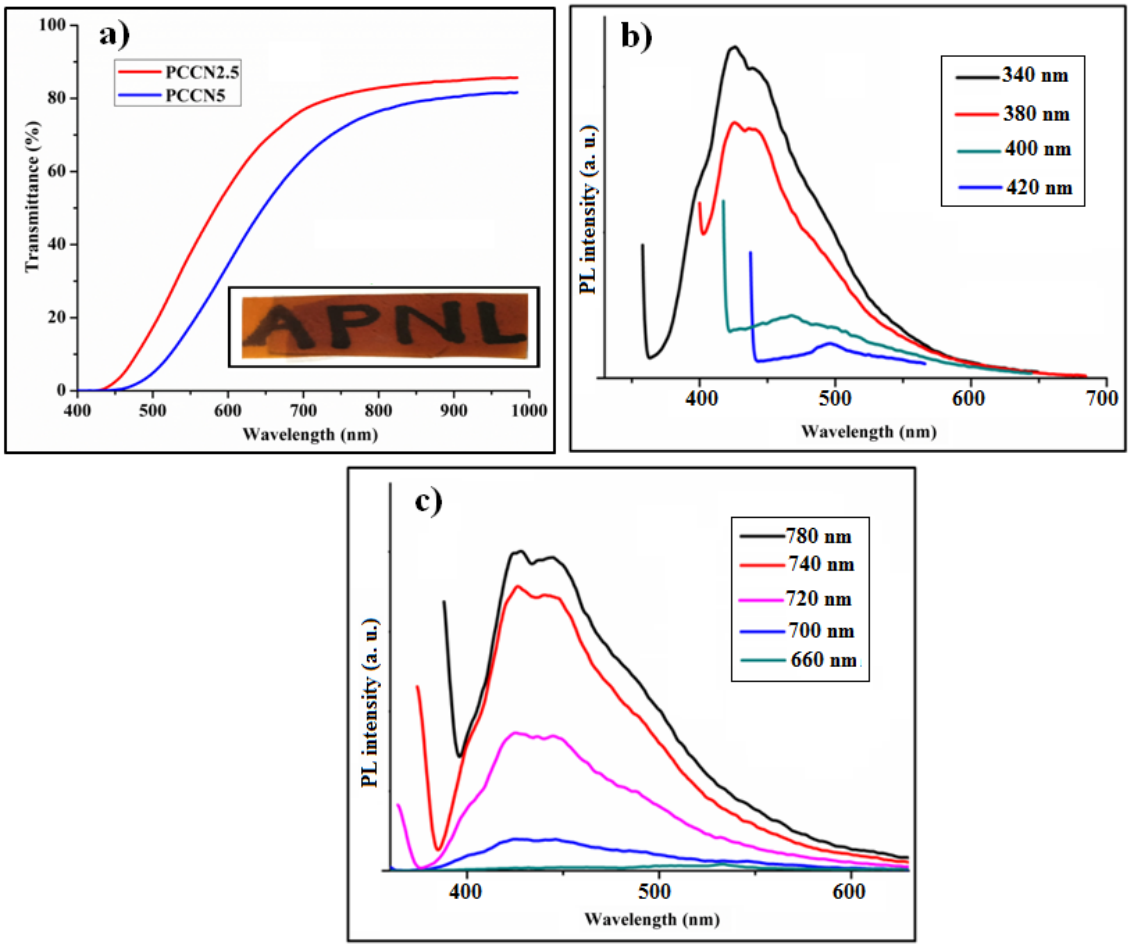

Figure 5.6: (a) Transmittance spectra of the thermosetting nanocomposite, and **(b and c)** wavelength dependent down- and up conversion PL spectra

5.3.8. Adsorption study of heavy metal ion

The nanocomposite was used for the removal of Pb(II) from the aqueous solution and the study was performed by monitoring the absorbance of the metal ion solution at different

time intervals during the adsorption study with the help of a UV-visible absorption spectroscopy. It is seen from the obtained values of absorbance that the nanocomposite was highly efficient in the removal of the metal ions. The removal efficiency (%) and adsorption capacity (mg g^{-1}) of Pb (II) were calculated using **Eq. 5.1** and **Eq. 5.2**, and the values were found to be 66% and 88 mg g^{-1} after 7h of exposure. Further, the adsorption of Pb (II) was checked in different pH (3-7) and the removal efficiency was found to be increased with the increase in pH values. The adsorption of metal ion as a function of initial pH played a significant role by clay-based nanocomposite. However, the adsorption increased with increasing solution pH, since more metal binding sites could be exposed with negative charges. Furthermore, different polar functional groups for example -OH, -COOH, $-NH_2$, etc. are present on the surface of the polymer nanocomposites. Thus, at lower pH, most of such functional groups are protonated and became positively charged, while at higher pH, they are deprotonated and transformed into negatively charged ions. Further, the H^+ and OH^- ions in solution may compete in the adsorption process [33, 34].

Further, the kinetics of the adsorption process was investigated in order to evaluate heavy metal ions removal efficiency of the nanocomposite from the polluted water. The effect of exposure time on the adsorption of Pb (II) was performed under ambient conditions. The results clearly reflect that the loading of nanohybrids significantly affect the adsorption of metal ions. The presence of high amount of nanohybrid in the nanocomposite facilitates in the rapid adsorption of heavy metal ions. The effective adsorption of metal ion might be attributed to two factors: one is strong interaction between metal ions and the functional groups present in the nanocomposite and other one is an electrostatic attraction between the freely exposed surface of the nanocomposite and the metal ions. The data obtained by the adsorption kinetics study (using equation **Eq. 5.3** and **Eq. 5.4**) are tabulated in **Table 5.2**. It is noticed from the observed data that pseudo-second order model fitted well with an excellent correlation coefficient for the adsorption of Pb (II) by the nanocomposite. In literature, adsorption kinetics of heavy metal ions onto the polymer nanocomposites were established to fit the pseudo-second order model, which indicated that the rate-limiting step in the removal of target metal ion by the polymer nanocomposites involved chemisorption owing to coordination, strong interaction, complexation, and/or chelation between sorbent and sorbate [35].

Further, the fitted constants for Freundlich and Langmuir models along with regression coefficients are summarized in **Table 5.3** that are obtained from **Figure 5.7a** and **5.7b** with the help of **Eq. 5.5** and **Eq. 5.6**. The isotherms and regression coefficients confirmed that the results fit better with the Langmuir model than with the Freundlich model. Literature also reported the adsorption isotherms were approximately fitted according to the Langmuir model in case of polymer-based nanocomposites [35]. Further, adsorption capacity for Pb(II) (90.9 mg g^{-1}) was found to be superior than clay-based polyaniline nanocomposite [34].

Table 5.2: Kinetic parameters of the nanocomposites obtained from different models

Nanocomposite	**Pseudo-first order**		**Pseudo-second order**	
	k_1	R^2	k_2	R^2
PCCN1	0.84	0.951	1.35	0.991
PCCN2.5	0.68	0.948	1.24	0.99
PCCN5	0.56	0.963	1.20	0.992

Further, one of the critical factors to gain a cost efficient heavy metal ion absorbent is the reusability of the nanocomposite for the adsorption of metal ions. The recycling of the nanocomposite was done just by filtering the pieces of films and washed several times with water. The efficiency is significantly good even after the third cycle of recycling (**Figure 5.7c**). This signifies that nanocomposite has good reusable capacity for removal of heavy metal ions. Therefore, the use of these materials is economically feasible for absorption of heavy metal ions.

Table 5.3: Isotherm constant for adsorption of Pb(II) by PCCN5 using Langmuir and Freundlich models

Langmuir constant			**Freundlich constant**		
q_e (mg g^{-1})	k_L (L mg^{-1})	R^2	k_F	n	R^2
90.9	0.06	0.9967	1.12	2.40	0.964

5.3.9: Photocatalytic degradation of dye

The photocatalytic ability of the nanocomposite was scrutinized by degrading model

organic dirt (RhB) under exposure of normal solar light. The representative plot of optical absorbance of the dye solution against wavelength for PCCN1 was recorded at different time intervals during the photodegradation process as shown in **Figure 5.8a**.

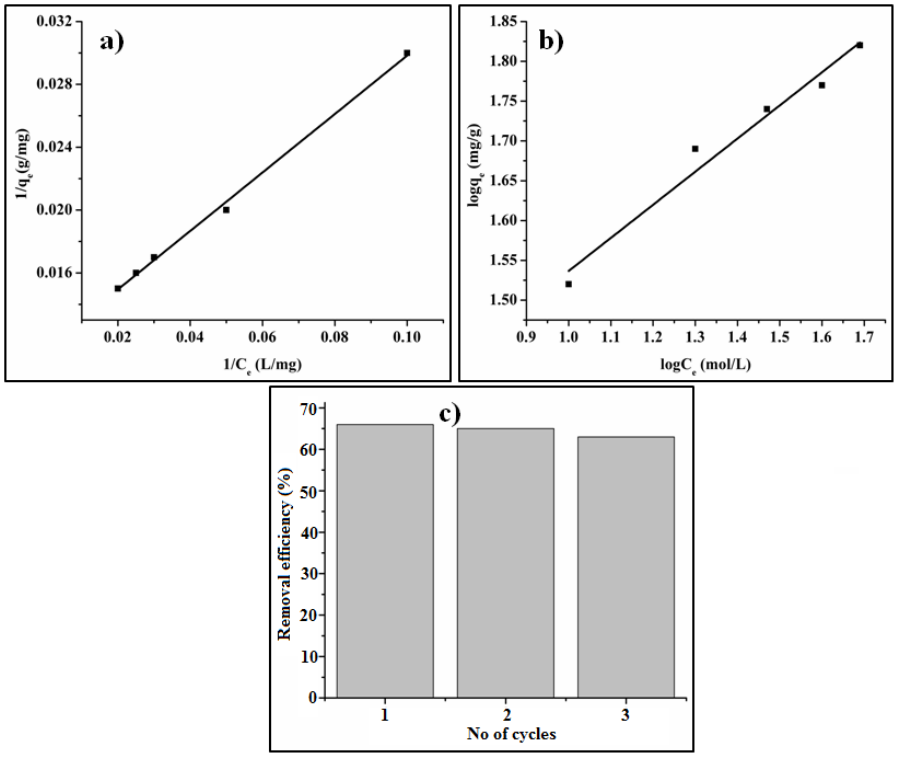

Figure 5.7: (a) Plot of $1/q_e$ *vs* $1/C_e$ (Langmuir isotherm), **(b)** plot of $\log q_e$ *vs* $\log C_e$ (Freundlich isotherm) and **(c)** recyclability of PCCN5

Further, the degradation efficiency of two different nanocomposites (PCCN1 and PCCN5) containing the lowest and the highest amount of nanohybrid after 420 min exposure of normal sunlight under ambient condition is provided in **Figure 5.8b**. The results demonstrated the significant degradation of dye by the nanocomposite in the presence of sunlight. Further, among the two different thermosets of the nanocomposite, PCCN5 showed the highest degradation efficiency (95%) after 6 h exposure of sunlight due to the presence of the highest amount of the nanohybrid. In case of this nanocomposite, clay was used as a support material of CD-based photocatalyst as the former possesses large pore volumes, high specific surface area, chemical stability and good mechanical properties. Dispersing CD onto the surface of clay mineral improves the photocatalytic activity by providing more active surface sites. Clay can reduce agglomeration and enhance the decomposition of organic and inorganic pollutants. Clay acts as a platform to facilitate the degradation process by electron hole pair mechanism

generated by CD present on the surface of clay upon exposure of light. Upon exposure of solar light, dye molecules adsorbed on clay can be potentially excited and an electron transport between the adsorbed dye molecules and the electron acceptor sites on the surface of clay might lead to a charge partition and subsequent development of dye radical cations. It is thus estimated that the created dye radical cations can undergo reactions with active oxygen species present within the system and lead to the decomposition of the dye molecule [36-39]. Furthermore, the kinetics of the degradation process was studied from the fitting plots of $\ln(C_0/C)$ against time (**Figure 5.8c**). The degradation of dye can be ascribed to pseudo first-order reaction with a simplified Langmuir-Hinshelwood model in accordance to the reported literature [22]. The rate constants of PCCN1 and PCCN5 were calculated by use of **Eq. 5.7** and the values were found to 5.4×10^{-3} min^{-1} and 7.1×10^{-3} min^{-1} for respectively. Similarly to the adsorption test, recyclability of the nanocomposite was also checked as a photocatalyst for degradation of organic contaminant. The degradation efficiency remained almost constant even after 3rd cycles of use (**Figure 5.8d**) and thus the nanocomposite has remarkable prospective as a reusable photocatalyst for degradation of organic pollutants.

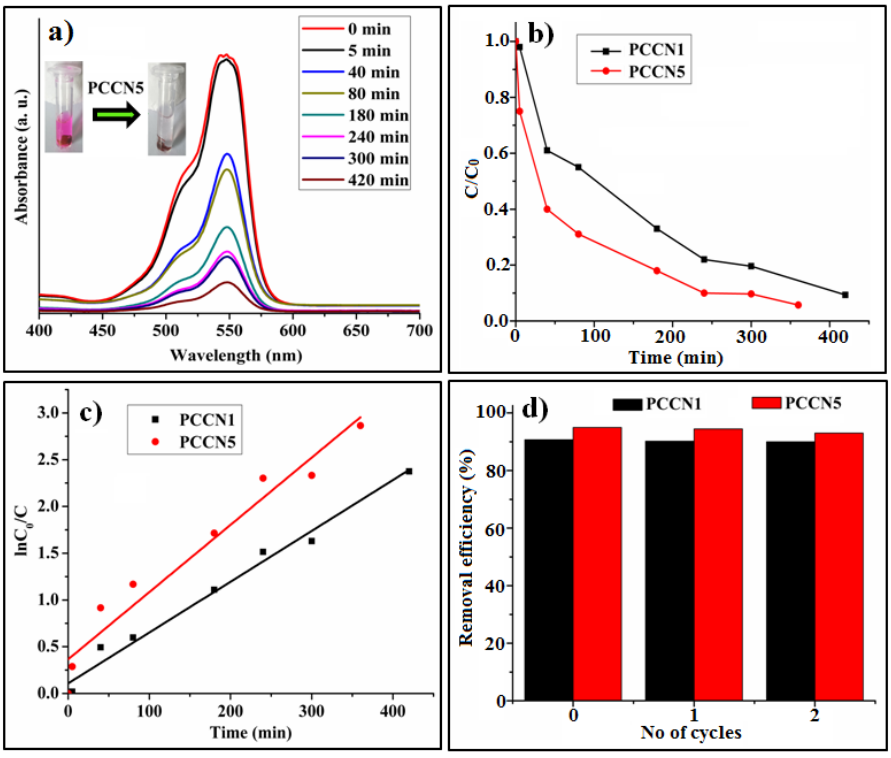

Figure 5.8: (a) UV-vis spectra of RhB with respect to time in presence of nanocomposite, **(b, c)** kinetics data plots for photocatalytic degradation and **(d)** removal **(%)** after recycling of the catalyst

5.4. Conclusion

In this present work, a clay@CD based WHPE nanocomposite was fabricated using bio-based raw materials by environmentally friendly approach. The nanocomposite showed tremendous enhancement in mechanical and thermal properties as well as in biodegradation behavior. Further, they also exhibited wavelength dependent both down- and up-conversion photoluminescence properties as well as excellent transparency. The nanocomposite possesses maximum adsorption capacities of 90.9 mg g^{-1} for the removal of Pb(II) ions in water. Further, this nanocomposite exhibits photocatalytic behavior for degradation of organic dirt like Rodamine B. This new nanocomposite is qualified for wastewater treatment as a low-cost, sustainable and effectual adsorbent.

References

[1] Aich, N., Tuttle, J. P., Lead, J. R., and Saleh, N. B. A critical review of nanohybrids: Synthesis, applications and environmental implications. *Environmental Chemistry*, 11(6):609-623, 2014.

[2] Banin, U., Shahar, B. Y., and Vinokurov, K. Semiconductor-metal nanoparticles: From architecture to function. *Chemistry of Materials*, 26(1):97-110, 2014.

[3] Zabihi, O., Ahmadi, M., Nikafshar, S., Preyeswary, C. K., and Naebe, M. A. Technical review on epoxy-clay nanocomposites: Structure, properties and their applications in fibre reinforced composites. *Composite Part B: Engineering*, 135:1-24, 2018.

[4] Krook, M., Albertsson, A. C., Gedde, U. W., and Hedenqvist, M. S. Barrier and mechanical properties of montmorillonite/polyesteramide nanocomposites. *Polymer Engineering and Science*, 42(6):1238-1246, 2002.

[5] Unuabonah, E. I. and Taubert, A. Clay-polymer nanocomposites (CPNs): Adsorbents of the future for water treatment. *Applied Clay Science*, 99:83-92, 2014.

[6] Tsai, T. Y., Li, C. H., Chang, C. H., Cheng, W. H., Hwang, C. L., and Wu, R. J. Preparation of exfoliated polyester/clay nanocomposites. *Advanced Materials*, 17(14):1769-1773.

[7] Schork, Q. S. F. J. and Deng, Y. Water-based polymer/clay nanocomposite suspension for improving water and moisture barrier in coating. *Composites Science and Technol*ogy, 67(9):1823-1829, 2007.

[8] Konwar, U., Mandal, M., and Karak, N. *Mesua ferrea* L. seed oil based acrylate-modified thermostable and biodegradable highly branched polyester resin/clay nanocomposites. *Progress in Organic Coatings,* 72(4):676-685, 2011.

[9] Lee, H. T., and Lin, L. H. Waterborne polyurethane/clay nanocomposites: Novel effects of the clay and its interlayer ions on the morphology and physical and electrical properties. *Macromolecules,* 39(18):6133-6141, 2006.

[10] Azeez, A. A., Rhee, K. Y., Park, S. J., and Hui, D. Epoxy clay nanocomposites – processing, properties and applications: A review. *Composite Part B: Engineering,* 45(1):308-320, 2013.

[11] Gaboune, A., Ray, S. S., Kadi, A. A., and Bousmina, B. R. M. Polyethylene/clay nanocomposites prepared by polymerization compounding method. *Journal of Nanoscience and Nanotechnology,* 6(2):530-535, 2006.

[12] Ollier, R., Rodriguez, E., and Alvarez, V. Unsaturated polyester/bentonite nanocomposites: Influence of clay modification on final performance. *Composites: Part A,* 48:137-143, 2013.

[13] Ratkievicius, L. A., Filho, F. J. V. C., Neto, E. L. D. B., and Santanna, V. C. Modification of bentonite clay by a cationic surfactant to be used as a viscosity enhancer in vegetable-oil-based drilling fluid. *Applied Clay Science,* 135:307-312, 2017.

[14] Zhang, Z., Sun, W., and Wu, P. Highly photoluminescent carbon dots derived from egg white: facile and green synthesis, photoluminescence properties, and multiple applications. *ACS Sustainable Chemistry & Engineering,* 3(7):1412-1418, 2015.

[15] Zhou, Y., Sharma, S. K., Peng, Z., and Leblanc, R. M. Polymers in carbon dots: A Review. *Polymers,* 9(2):1-20, 2017.

[16] Konwar, U., Karak, N., and Mandal M. *Mesua ferrea* L. seed oil based highly thermostable and biodegradable polyester/clay nanocomposites. *Polymer Degradation and Stability,* 94(12):2221-2230, 2009.

[17] Decker, J. J., Chvalun, S. N., and Nazarenko, S. Intercalation behavior of hydroxylated dendritic polyesters in polymer clay nanocomposites prepared from aqueous solution. *Polymer,* 52(18):3943-3955, 2011.

[18] Lee, S. R., Park, H. M., Lim, H., Kang, T., Li, X., Cho, W. J., and Ha, C. S. Microstructure, tensile properties and biodegradability of aliphatic polyester/clay nanocomposite. *Polymer,* 43(8*)*:2495-2500, 2002.

[19] Venkateswarlu, S., Panda, A., Kim, E., and Yoon, M. Biopolymer-coated magnetite nanoparticles and metal–organic framework ternary composites for cooperative Pb(II) adsorption. *ACS Applied Nano Materials*, 1(8):4198-4210, 2018.

[20] Cao, C. Y., Qu, J., Yan, W. S., Zhu, J. F., Wu, Z. Y., and Song, G. Low-Cost Synthesis of flowerlike α-Fe_2O_3 nanostructures for heavy metal ion removal: Adsorption property and mechanism. *Langmuir*, 28(9):4573-4579, 2012.

[21] Wang, J., Zhang, S., Shao, Y., Liu, J., Xu, Z., and Zhu, D. A. Amino functionalized Fe_3O_4@SiO_2 core-shell magnetic nanomaterials as a novel adsorbent for aqueous heavy metal ion removal. *Journal of Colloid & Interfac Science*, 349(1):293-299, 2010.

[22] Thakur, S., Das, G., Raul, P. K., and Karak, N. Green one-step approach to prepare sulfur/reduced graphene oxide nanohybrid for effective mercury ions removal. *Journal of Physical Chemistry C*, 117(15):7636-7642, 2013.

[23] Solener, M., Tunali, S., Ozcan, A. S., Ozcan, A., and Gedikbey, T. Adsorption characteristics of lead(II) ions onto the clay/poly(methoxyethyl)acrylamide (PMEA) composite from aqueous solutions. *Desalination*, 223(1-3):308-322, 2008.

[24] Li, J., Chen, C., Zhao, Y., Hu, J., Shao, D., and Wang, X. Synthesis of water-dispersible Fe_3O_4@β-cyclodextrin by plasma-induced grafting technique for pollutant treatment. *Chemical Engineering Journal*, 229:296-303, 2013.

[25] Hazarika, D. and Karak, N. Photocatalytic degradation of organic contaminants under solar light using carbon dot/titanium dioxide nanohybrid, obtained through a facile approach. *Applied Surface Scien*ce, 376:276-285, 2016.

[26] Gungor, N. and Karaoglan, S. Interactions of polyacrylamide polymer with bentonite in aqueous systems. *Materials Letters*, 48(3-4):168-175, 2001.

[27] Dalir, H., Farahani, R. D., Nhim, V., Samson, B., Levesque, M., and Therriault, D. Preparation of highly exfoliated polyester-clay nanocomposites: Process-property correlations. *Langmuir*, 28(1):791-803, 2012.

[28] Maji, P. K., Guchhait, P. K., and Bhowmick, A. K. Effect of nanoclays on physico-mechanical properties and adhesion of polyester-based polyurethane nanocomposites: structure-property correlations. *Journal of Materials Science*, 44(21):5861-5871, 2009.

[29] Xu, Y., Ren, X., and Hanna, M. A. Chitosan/clay nanocomposite film preparation and characterization. *Journal of Applied Polymer Science*, 99(4):1684-1691, 2006.

[30] Chakardhar, K. V. P.; Subbaiah, K. V.; Kumar, M. A.; Reddy, G. R. Blended epoxy/polyester polymer nanocomposite: Effect of "nano" on mechanical properties. *Polymer-Platics Technology and Engineering*, 51(1):92-96, 2012.

[31] De, B., Gupta, K., Mandal, M., and Karak, N. Biocide immobilized OMMT-carbon dot reduced Cu_2O nanohybrid/hyperbranched epoxy nanocomposites: Mechanical, thermal, antimicrobial and optical properties. *Materials Science and Engineering: C*, 56:74-83, 2015.

[32] Koo, C. M., Ham, H. T., Choi, M. H., Kim, S. O., and Chung, I. J. Characteristics of polyvinylpyrrolidone-layered silicate nanocomposites prepared by attrition ball milling. *Polymer*, 44(3):681-689, 2003.

[33] Chen, L. F., Liang, H. W., Lu, Y., Cui, C. H., and Yu S. H. Synthesis of an attapulgite clay@carbon nanocomposite adsorbent by a hydrothermal carbonization process and their application in the removal of toxic metal ions from water. *Langmuir*, 27(14):8998-9004, 2011.

[34] Piri, S., Zanjani, Z. A., Piri, F., Zamani, A., Yaftian, M., and Davari, M. Potential of polyaniline modified clay nanocomposite as a selective decontamination adsorbent for Pb(II) ions from contaminated waters; kinetics and thermodynamic study. *Journal of Environmental Health Science & Engineering*, 14(1):20, 2016.

[35] Zhang, Q., Pan, B., Zhang, S., Wang, J., Zhang, W., and Lv, L. New insights into nanocomposite adsorbents for water treatment: A case study of polystyrene-supported zirconium phosphate nanoparticles for lead removal. *Journal of Nanoparticle Research*, 13(10):5355-5364, 2011.

[36] Li, L., Fan, L., Sun, M., Qiu, H., Li, X., Duan, H., and Luo, C. Adsorbent for chromium removal based on graphene oxide functionalized with magnetic cyclodextrin-chitosan. *Colloids and Surfaces B: Biointerfaces*, 107:76-83, 2013.

[37] Zhang, Z. H., Yu, Y. J., and Wang, P. Hierarchical top-porous/bottom-tubular TiO_2 nanostructures decorated with Pd nanoparticles for efficient photoelectrocatalytic decomposition of synergistic pollutants. *ACS Applied Materials & Interfaces*, 4(2):990-996, 2012.

[38] Zhang, Z. H. and Wang, P. Optimization of photoelectrochemical water splitting performance on hierarchical TiO_2 nanotube arrays. *Energy & Environmental Science*, 5(4):6506-6512, 2012.

[39] Fang, Y., Zhou, A., Yang, W., Araya, T., Huang, Y., Zhao, P., Johnson, D., Wang, J., and Ren, Z. J. Complex formation via hydrogen bonding between Rhodamine B and montmorillonite in aqueous Solution. *Scientific Reports*, 8(1):229, 2017.